Functional Characterization of the Protease of Human Endogenous Retrovirus, K10: Can It Complement HIV-1 Protease?†

Eric M. Towler,*,‡,§,⊥ Sergei V. Gulnik,§,|| T. N. Bhat,|| Dong Xie,|| Elena Gustschina,|| Terry R. Sumpter,‡ Nicole Robertson,⊥ Christopher Jones,⊥ Marlies Sauter,@ Nikolaus Mueller-Lantzsch,@ Christine Debouck,⊥ and John W. Erickson||

Protein Chemistry Laboratory and Structural Biochemistry Program, SAIC Frederick, NCI-FCRDC, P.O. Box B, Frederick, Maryland 21702, Department of Molecular Genetics, SmithKline Beecham Pharmaceuticals, 709 Swedeland Road, King of Prussia, Pennsylvania 19406, and Abteilung Virologie, Institute Medizinische Mikrobiologie und Hygiene, Haus 47, Universitätskliniken des Saarlandes, 66421 Homburg/Saar, Germany

Received August 6, 1998; Revised Manuscript Received October 5, 1998

ABSTRACT: To investigate the biochemical properties of the protease encoded by the human endogenous retrovirus, K10 (HERV-K), 213 amino acids of the 3′-end of the HERV-K protease (PR) open reading frame were expressed in *Escherichia coli*. Autocatalytic cleavage of the expressed polypeptide resulted in an 18.2 kDa protein which was shown to be proteolytically active against a fluorogenic peptide used as a substrate for HIV-1 protease. On the basis of sequence homology and molecular modeling, the 106 N-terminal amino acids of HERV-K PR were predicted to comprise a retroviral protease core domain. An 11.6 kDa protein corresponding to this region was expressed and shown to be a fully functional enzyme. The 11.6 kDa domain of HERV-K PR is unusually stable over a wide pH range, exhibits optimal catalytic activity between pH 4.0 and 5.0, and exists as a dimer at pH 7.0 with a K_d of 50 μM. Like HIV-1 PR, the HERV-K PR core domain is activated by high salt concentrations and processes HIV-1 matrix-capsid polyprotein at the authentic HIV-1 PR recognition site. However, both the 18.2 and 11.6 kDa forms of HERV-K PR were highly resistant to a number of clinically useful HIV-1 PR inhibitors, including ritonavir, indinavir, and saquinavir. This raises the possibility that HERV-K PR may complement HIV-1 PR during infection, and could have implications for protease inhibitor therapy and drug resistance.

The human endogenous retrovirus, type K (HERV-K), represents the biologically most active form of a variety of retroelements present in the human genome (*1*, *2*). Having no known taxonomy, the HERV-K virus was named according to its use of lysyl-tRNA as a primer for its reverse transcriptase, thus the "type K" designation. Although present at 30−50 copies per genome, no complete HERV-K provirus has been identified (*3*). Like other retroviruses, the HERV-K genome encodes a putative aspartic PR (*3*). Similar to type B retroviruses, the HERV-K PR gene is situated between *gag* and *pol* in its own open reading frame (ORF) (*4*). In a previous report (*5*), it was shown that a recombinant protein corresponding to the HERV-K PR gene product autoprocessed to a smaller protein of approximately 18 kDa.

HERV-K proviral genes are expressed in a variety of tissues under both normal and pathophysiological conditions (*1*, *6*). In one study, expression of the HERV-K envelope protein was detected in the blood of 70% of HIV-1-infected individuals in contrast to only 3% of normal individuals (*1*). HERV-K gene expression results in the production of noninfectious virus-like particles that apparently package active reverse transcriptase (*7*) and a functional PR (*8*). The active expression of HERV-K proteins in HIV-1-infected individuals raises the possibility that HERV-K PR may be able to modulate HIV-1 PR function through interactions with HIV-1 PR substrates or inhibitors. In this report, we demonstrate that the HERV-K PR gene encodes a retroviral protease core domain that possesses catalytic activity comparable to that of HIV-1 protease, recognizes and authentically cleaves HIV-1 matrix-capsid polyprotein, and is highly resistant to potent HIV-1 protease inhibitors. Our results are discussed in terms of viral resistance and raise the interesting possibility that HERV-K PR may complement HIV-1 PR in drug-treated cells.

MATERIALS AND METHODS

Escherichia coli Strains and Molecular Biological Techniques. Standard molecular biology techniques were used for the production and handling of DNA and bacteria (*9*). The *E. coli* expression strain LW29(DE3) was kindly provided by Lisa A. Wysocki (Department of Biological Process Sciences, SmithKline Beecham). Briefly, LW29-(DE3) was constructed by transducing W3110 (ATCC 27325) with a P1 stock of CY15070 (ATCC 47022) to create a lacIq derivative and subsequently lysogenized with λ DE3 using the Novagen lysogenization kit. DNA restriction enzymes were purchased from Gibco-BRL (Gaithersburg,

† Supported in part by NIH Grant R01 GM50579.

* To whom correspondence should be addressed. E-mail: towlere@ncifcrf.gov. Fax: (301) 846-6321.

‡ Protein Chemistry Laboratory, NCI-FCRDC.

§ These authors contributed equally to this work.

|| Structural Biochemistry Program, NCI-FCRDC.

⊥ SmithKline Beecham Pharmaceuticals.

@ Universitätskliniken des Saarlandes.

10.1021/bi9818927 CCC: $15.00
Published on Web 11/12/1998

MD). The DNA sequence was confirmed by ABI automated sequencing. Site-directed mutagenesis was performed using the QuickChange Site-Directed Mutagenesis Kit (Stratagene) according to the manufacturer's recommendations. All other reagents were enzyme grade and were provided by various suppliers. In carrying out plasmid construction, mutagenesis, and sequence comparisons, we were assisted by the GCG program package (*10*).

Cloning and Expression of HERV-K PRs. *PR213::His6 and PR163*. The HERV-K PR open reading frame was amplified by polymerase chain reaction (PCR) with Taq polymerase (Perkin-Elmer) from pKP1.3 (*5*) using the primers 5′-CCC CGG GTG ACT ATA AAG GCG AAA TTC-3′ and 5′-GTC GAC GCT CTA CAG TGA CCG CCC CTA-3′. The *Xma*I−*Sal*I digest of the resulting PCR fragment was cloned into the *E. coli* expression vector pEMT15 (*11*), which provides the amino-terminal galactokinase tag. The *Nde*I−*Sal*I digest of this clone was subcloned into pET22b (Novagen, Inc.). To engineer the His_6 tag on the C terminus, the insert was reamplified by PCR using the primers 5′-TAA TAC GAC TCA CTA TAG-3′ and 5′-GGG CTC GAG AAA AGG ATA CCC TAT TCC TTC TCT TTC-3′, digested with *Nde*I−*Xho*I, and cloned into pET21a-(+), creating *PR213::His6*. The truncated form of the protease, *PR163*, and active site mutants were created using the Quick-Change mutagenesis kit as described above.

Protein expression in LW29(DE3) was induced by 1 mM IPTG for 1 h at 37 °C. Protein expression was detected by Western analysis using rabbit anti-PR antibodies (*5*) and the enhanced chemiluminescence kit (Amersham) according to the manufacturer's instructions.

Purification of the Proteases. The 18.2 kDa form of the PR was purified as follows. The cell pellet was resuspended in 10 mL of PO_4/0 buffer [20 mM sodium PO_4/2 mM EDTA/5 mM DTT (pH 7.0)] per gram of cell paste. Leupeptin and PMSF were added to final concentrations of 2 and 1 mM, respectively. Cells were lysed by eight 30 s pulses with a Branson sonicator at 50% maximum power. The lysate was spun for 30 min at 20 K in a Beckman JA-12 rotor. The soluble lysate was applied to S-Sepharose FF (Pharmacia) at 30 cm/h and washed with 10 column volumes of PO_4/0 buffer. The PR was eluted in 1 column volume with PO_4/100 (PO_4/0 buffer adjusted to 100 mM NaCl). The pooled fractions were applied directly to Q-Sepharose FF (Pharmacia) at 120 cm/h and washed with 1 column volume of PO_4/100. To the flow through and wash fractions of Q-Sepharose FF was added an equal volume of Phenyl/B buffer [PO_4/100 adjusted to 2 M $(NH_4)_2SO_4$]. The sample was applied to Phenyl-Superose (Pharmacia) at 2.5 cm/h and washed with 10 column volumes of 50% Phenyl/B and 50% PO_4/100. The PR was eluted with a linear gradient of 50% A/50% B to 100%A/0% B over 10 column volumes, where buffer A was PO_4/100 and buffer B was Phenyl/B. The PR eluted as a single band on a Coomassie gel at about 20% B. The yield was approximately 0.1−0.3 mg per 3−4 g of wet cell paste. Fractions were frozen on dry ice and stored at −80 °C.

The 11.6 kDa form of the PR was purified as follows. The cell paste was resuspended in 5 mL of Q/0 buffer [50 mM Tris-HCl/5mM EDTA/5 mM DTT (pH 8.0)] per gram of cell paste. PMSF and leupeptin were added to concentrations 1 and 2 mM, respectively. Cells were lysed by sonication as above or by one pass through an Avestin high-pressure homogenizer (Avestin, Inc.) at 12 000 psi. The cell lysate was spun for 30 min at 20 000 rpm in a Beckman JA-12 rotor. To the soluble was added lysate 225 g of $(NH_4)_2SO_4$ per liter to a final concentration of 37.5% saturation. This was stirred for 30 min at 4 °C and spun for 30 min at 10 000 rpm in a Beckman JA-12 rotor. The supernatant was collected, and 144 g of $(NH_4)_2SO_4$ per liter was added to adjust the solution to 60% saturation. This was stirred for 30 min at 4 °C, and the centrifugation was repeated. The pellet was resuspend in Q/0 buffer and dialyzed extensively against the same buffer. The soluble dialysate was applied to Q-Sepharose FF (Pharmacia) at 30 cm/h. The column was washed with 5 column volumes of Q/0 buffer, and the PR was eluted with a NaCl salt gradient. The PR eluted at about 150−200 mM NaCl. The peak fractions were pooled, concentrated by an Amicon filter (Amicon), and applied to a Superose 12 column (Pharmacia) equilibrated in Q/200 buffer (Q/0 adjusted to 200 mM NaCl) at 15 cm/h. The PR-containing peak was collected, reconcentrated, and reapplied to the Superose 12 column. After the second run of the Superose 12 column, the PR-containing peak was collected. The PR was frozen at −80 °C.

HIV-1 PR was expressed in *E. coli* and purified from inclusion bodies as described previously (*12*).

Mass Spectrometry. Matrix-assisted laser desorption ionization mass spectrometry (MALDI-MS) data were obtained on a PerSeptive Biosystems Voyager RP laser desorption time-of-flight mass spectrometer. Protein samples were prepared for analysis by diluting analyte 1:5 with 3,5-dimethoxy-4-hydroxycinnamic acid (10 mg/mL in 2:1 0.1% trifluoroacetic acid/acetonitrile) for a final concentration of 1−10 pmol/μL. Bovine β-lactoglobulin A (Sigma) was included as an internal calibrant (MH^+ 18 364 Da). Desorption or ionization was accomplished using photon irradiation from a 337 nm pulsed nitrogen laser and a 25 keV accelerating energy. Spectra were averaged over ca. 100 laser scans.

N-Terminal Sequence Analysis. Sequence analysis was performed on a Beckman LC-3400 Tri-Cart gas-phase protein sequencer equipped with a Beckman 126/166 system for on-line PTH analysis. Data were acquired using System Gold chromatography software. Samples were electroblotted onto PVDF type supports (Problott), and standard Beckman optimized PVDF sequencing cycles were used.

Enzyme Kinetics. Protease activity and K_i's were measured essentially as described previously (*13*) using the fluorogenic substrate Lys-Ala-Arg-Val-Tyr-Phe(NO_2)-Glu-Ala-Nle-NH_2 (*14*). Excitation and emission maxima were 277 and 306 nm, respectively. To determine active enzyme concentrations, active site titrations were performed in the presence of 1.25 ammonium sulfate either at pH 8.0 for HERV-K PR, using the inhibitor KNI-227, or at pH 6.2 for HIV-1 PR, using the inhibitor KNI-227 or ABT-538. These conditions were selected to provide optimal [substrate]/K_m ratios. Kinetic constants were determined at pH 4.5 and 1 M NaCl.

Effect of pH on the Activity and Stability of Proteases. To determine the pH optimum of activity, activity of enzymes against fluorogenic substrate was measured at pH 3.0−8.0 in following buffers at 50 mM concentrations: pH 3.0−3.5, Gly-HCl; pH 4.0−5.5, sodium acetate; pH 6.1−7.5, PIPES/NaOH; pH 8.0−8.5, Tris-HCl; and pH 9.0, AMPSO. All

A.

```
1                                                  50 51                                                  100
 HIV-1   ~~~~~~~~~~ ~~~~~~~~~~ ~~~~~~~~~~ ~~~~~~~~~~ ~~~~~~~~~~ ~~~~~~~~~~ ~~~~~~~~~~ ~~~~~~~~~~ ~~~~~~~~~~
HERV-K10 KWATIVGKRA KGPASGPTTN WGIPNSAICS SGFSGTTTPT VPSVSGNKPV TTIQQLSLTT SGSAAVDLCT IQAVSLLPGE PPQKIPTGVY GPLPEGTVGL

         101                                       150 151                                               200
 HIV-1   ~~~~~~~~~~ ~~~~~~~~~~ ~~~~~~~~~~ ~~~~~~~~~~ ~~~~~~~~~~ ~~~~~~~~~~ ~~~~~~~~~~ ~~~~~~~~~~P QITLWQRPLV TIKIGGQLKE
HERV-K10 ILGRSSLNLK GVQIHTSVVD SDYKGEIQLV ISSSIPWiAc PgDRIAQLLL LPYIKGGNSE lKkIGGLgST DPTGKAAYWA SQVSENRPVC KAIIQGKQFE

         201*                                      250 251                                               300
 HIV-1   ALLDTGADDT VLEEMSLPGR WKPKM....I GGIGGFIKVR QYDQILIEIC GHKAIGTV.. LVGPTPVNII GRNLLTQIGC TLNF~~~~~~ ~~~~~~~~~~
HERV-K10 GLVDTGADVS IIALNQWPKN WPKQKAVTGL VGIGTASEVY QStEILHCLG PDNQESTVQP MITSIPLNLW GRDLLQQWGA EITMPAPLYS PTSQKIMTKr

         301                                 335
 HIV-1   ~~~~~~~~~~ ~~~~~~~~~~ ~~~~~~~~~~ ~~~~~
HERV-K10 GYIPGKGLGK NEDGIKiPfE AKINQEREGI GYPF-(LEHHHHHH)
```

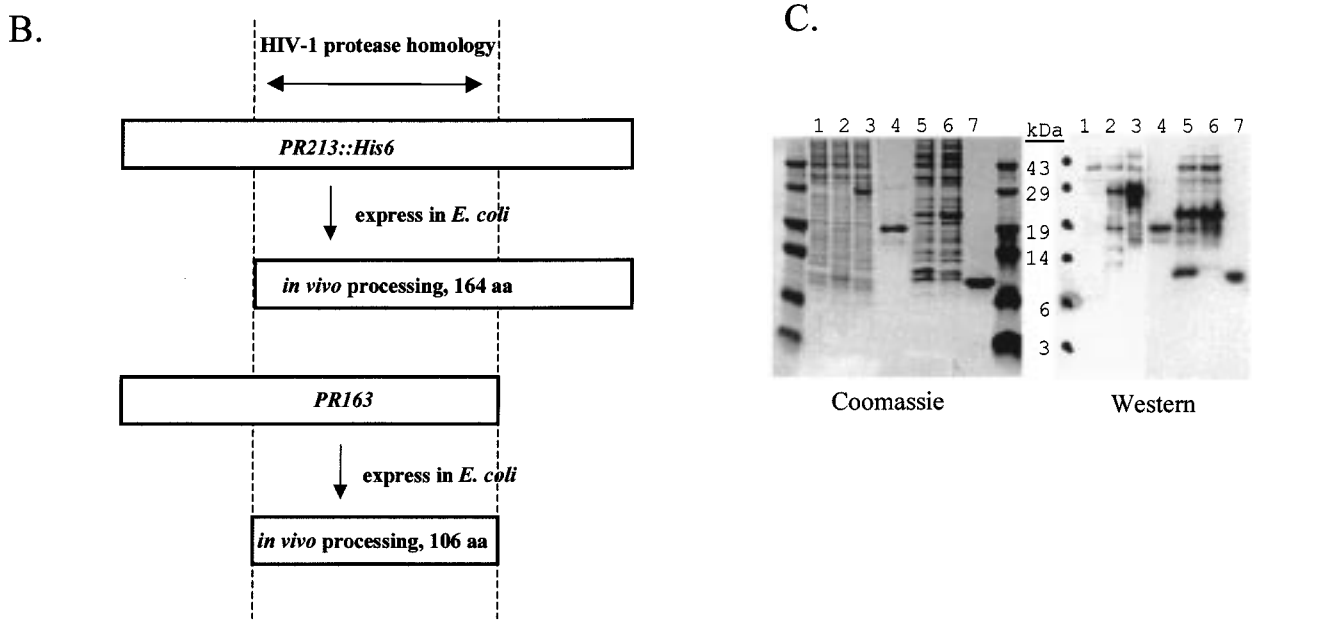

FIGURE 1: Expression and purification of HERV-K PR and its relationship to HIV-1 PR. (A) Sequence alignment of the entire HERV-K10 PR ORF and mature HIV-1 PR using the program PILEUP (*10*). Deviations from the published sequence for the HERV-K PR ORF (*3*) which likely reflect clonal variation are denoted by lowercase letters. Insertions are denoted by a period (".") in the alignment. The underlined sequence represents the portion of the ORF present in clone *PR213::His6*. The D-T-G signature motif of aspartic proteases is boxed, and the conserved catalytic aspartic acid in HERV-K PR that was mutated to a methionine is indicated with an asterisk. The sequence of the engineered His_6 tag is shown in parentheses. The arrow indicates the N-terminal cleavage site. (B) Schematic representation of HERV-K PR expression constructs. (C) A 16% SDS−PAGE of equivalent amounts of protein from whole cell lysates or purified PR: lane 1, control strain; lane 2, strain expressing the precursor of the 18.2 kDa form of the PR (*PR213::His6*); lane 3, strain expressing the precursor of the 18.2 kDa form of the PR with an active site mutation; lane 4, approximately 2 μg of the purified 18.2 kDa PR; lane 5, strain expressing the precursor of the 11.6 kDa form of the PR (*PR163*); lane 6, strain expressing the precursor of the 11.6 kDa form of the PR with an active site mutation; and lane 7, approximately 6 μg of the purified 11.6 kDa PR. At left is the Coomassie-stained gel; at right is the Western blot using rabbit anti-HERV-K10 PR polyclonal antibodies (*5*).

buffers contained 1 mM EDTA, 0.05% PEG-8000, and 2 mM DTT. The final concentrations of proteases were 15 and 31 nM for HIV-1 and HERV-K10 PR, respectively. To determine the pH optimum of stability, enzymes were incubated for 1−24 h in indicated buffers at concentrations of 0.35 mg/mL, and the remaining activity was then measured at pH 6.2 in the presence of 1.25 M ammonium sulfate.

p17−p24 Cleavage. HIV-1 matrix-capsid protein was expressed and purified as proposed by H. Wang (unpublished). For the cleavage study, it was incubated at 1 mg/mL in 50 mM MES/NaOH buffer (pH 6.0) with the respective proteases for 10−300 min at 37 °C. The enzyme:substrate molar ratio was 1:53 and 1:2670 for HERV-K and HIV-1 PRs, respectively. The reaction was stopped by the addition of 5× SDS sample buffer and analyzed using an 8 to 25% gradient SDS−PAGE.

Analytical Centrifugation. Equilibrium sedimentation experiments were performed using a Beckman model XL-A analytical ultracentrifuge. The calculated monomer molecular mass and extinction coefficient at 280 nm were 11 646 Da and 29 970 M^{-1} cm^{-1}, respectively. Sedimentation experiments were carried out at 4 °C in 20 mM sodium phosphate buffer (pH 7.0) containing 0.2 M NaCl. Three data sets were collected for each of two different protein concentrations, 0.08 and 0.23 mg/mL, at rotor speeds of 21 000, 24 000, and 27 000 rpm after reaching equilibrium. The data were subjected to a global analysis using a nonlinear least-squares program (*15*) provided by the manufacturer. A partial specific volume of 0.74 mL/g was calculated on the basis of the amino acid composition for HERV-K PR (*16*). The solvent density was measured using a pyncnometer (Mettler Instruments Co.).

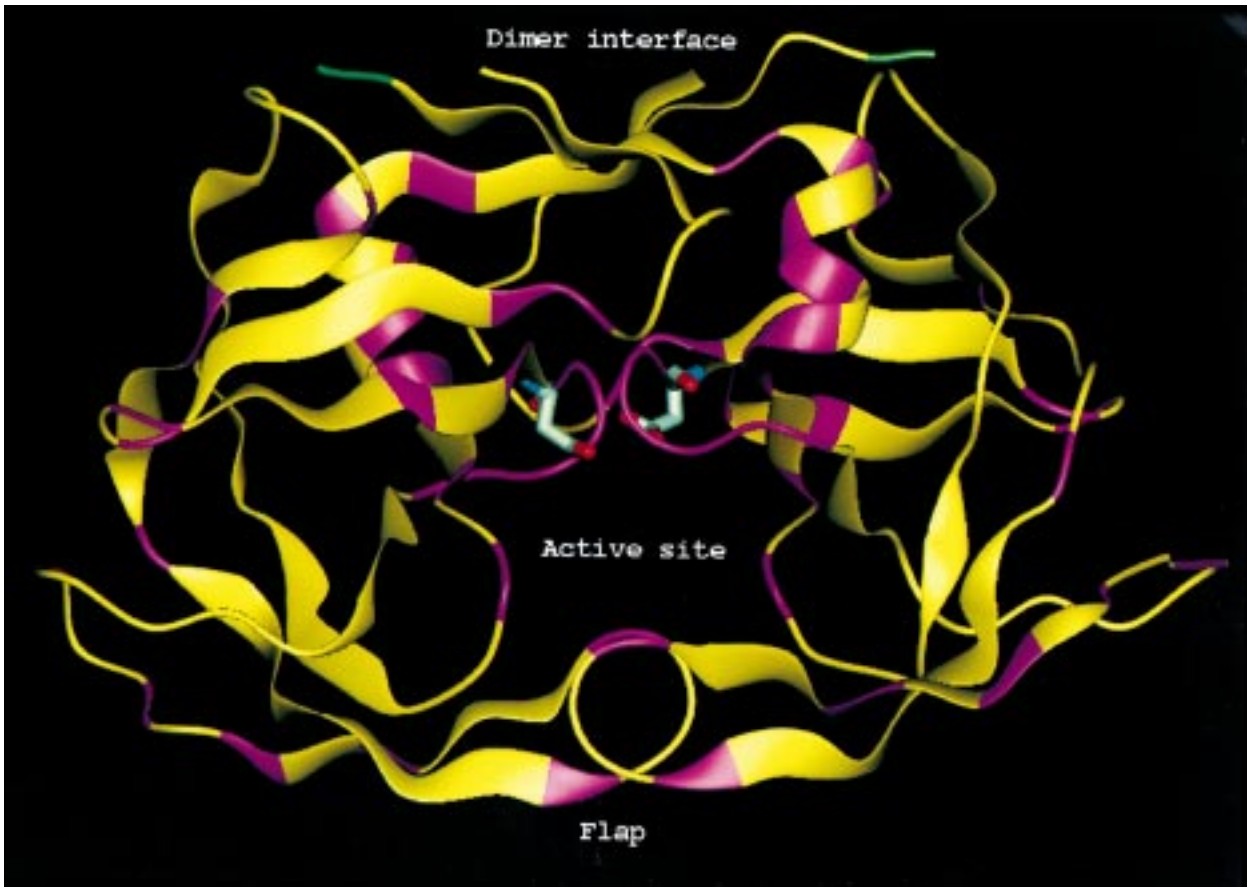

FIGURE 2: Ribbon diagram of the three-dimensional model of HERV-K PR. Coordinates of the structure of HIV-1 PR−KNI-272 complex (*26*) were used as a template for modeling the substitutions of the homologous core domain (residues 1−106) of HERV-K PR using the program LOOK (*27*). Regions with identical sequences are magenta. The beginning of the C-terminal extension is green.

RESULTS AND DISCUSSION

Identification of Catalytically Active Forms of HERV-K PR. The HERV-K PR ORF encodes a protein that is 28% identical to HIV PR over a 106-residue region and includes a D-T-G motif that is the signature sequence of aspartic proteases (Figure 1A). HIV PR is autoprocessed at both the N and C termini of its polyprotein precursor to form mature enzyme. Since the autoprocessing sites of HERV-K PR were unknown, a 213-amino acid region of the HERV-K PR ORF that encodes a protein extending from 58 residues N-terminal to the HIV-1 PR homology region through the ORF stop codon was cloned into a pET21 vector. A galK sequence tag was engineered into the N terminus to increase the extent of *E. coli* expression of soluble protein (*17*), and a hexahistidine tag (His_6) was engineered into the C terminus, creating the construct *PR213::His6* (Figure 1B). Consistent with previous results (*5*), the ORF-encoded product autoprocessed to a protein that migrated as an 18 kDa species on SDS−PAGE (Figure 1C, lane 2). The functional role of the putative catalytic aspartic acid at position 26 in the 18 kDa protein was demonstrated by the fact that a D26M active site mutation resulted in a protein that was incapable of autoprocessing (Figure 1C, lane 3). N-Terminal sequencing and mass spectroscopy of the purified 18 kDa protein demonstrated that autoprocessing occurred only at the sequence KAAY−WASQ (where Y−W represents the scissile bond) and resulted in a 164-amino acid protein with a molecular mass of 18 230 Da. The mass is consistent with that predicted from the amino acid sequence assuming the presence of the engineered His_6 tag at the C terminus.

Retroviral proteases range in length from 99 to 125 residues, but the N- and C-terminal strands that form the intersubunit β-sheet are structurally conserved (*18*). On the basis of sequence alignment analysis, the 18.2 kDa form of HERV-K PR protein was predicted to contain a 50-amino acid extension (not including the engineered His_6 tag) relative to the mature carboxy terminus of HIV-1 PR (Figure 1A). A three-dimensional atomic model of the first 106 residues of the HERV-K PR was constructed using the program LOOK (Figure 2). Besides the active site aspartic acids and the C-terminal α-helix, residues in and around the active site region tend to be more highly conserved than those in outer segments, including the flaps. Although the residues of the N- and C-terminal strands, which stabilize the dimer interface, are not well-conserved, they form a plausible antiparallel β-sheet with good geometry and complementary side chain packing. Thus, the modeling analysis predicted that a functional homodimeric enzyme can be constructed from the first 106 residues of the 18.2 kDa form of HERV-K PR.

To confirm this prediction, a stop codon was inserted into the *PR214::His6* construct to produce a protein terminating at Met106 of the 18.2 kDa protein (*PR163*) (Figure 1B). Expression of *PR163* in *E. coli* resulted in an autoprocessed protein of approximately 12 kDa as predicted (Figure 1C, lane 5). As with the original *PR214::His6* construct, the active site D26M mutation eliminated autoprocessing (Figure

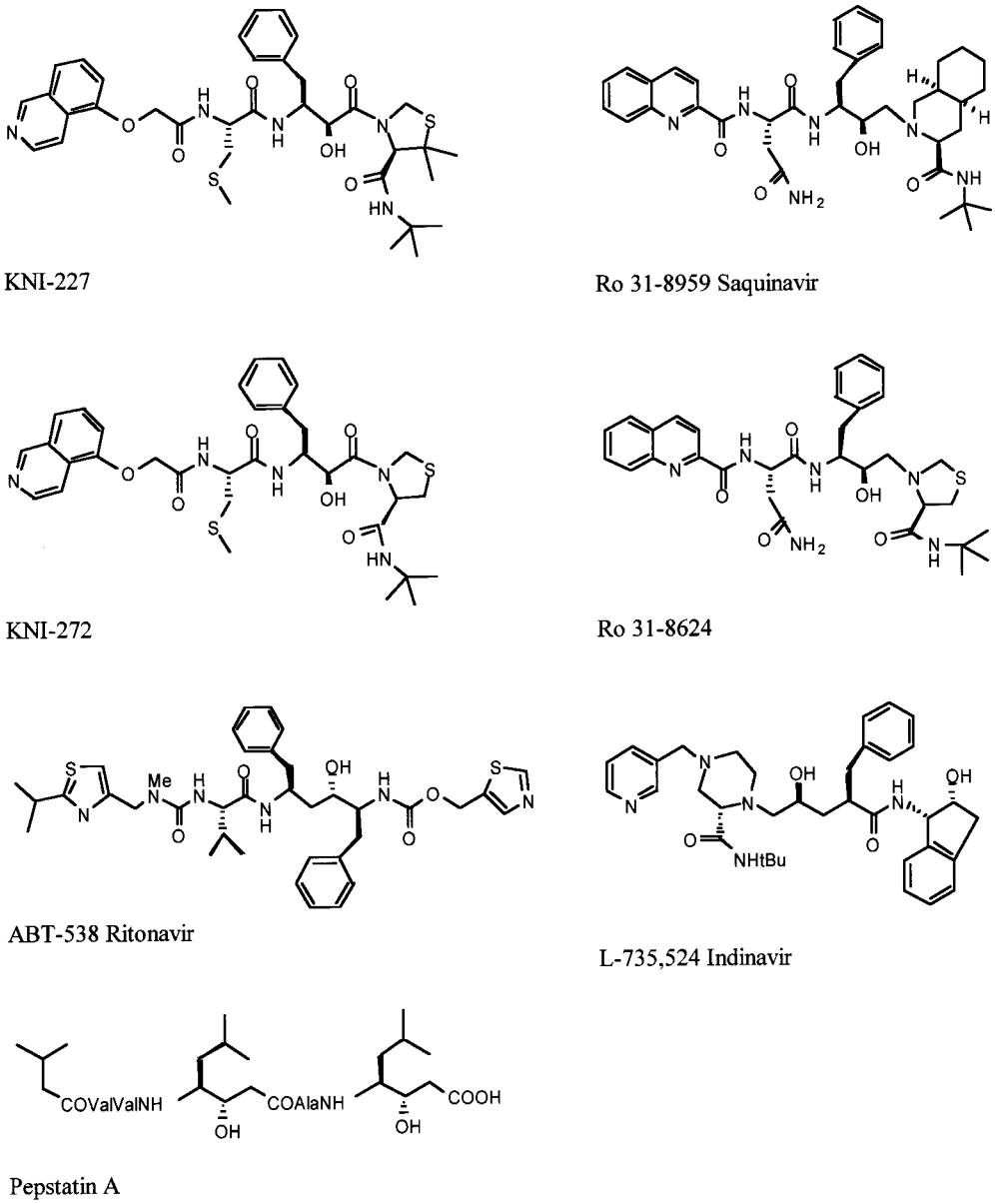

FIGURE 3: Chemical structures of inhibitors used in this study.

Table 1: Kinetic Constants of Peptide Substrate Cleavage

protease	K_m (μM)	k_{cat} (s^{-1})	k_{cat}/K_m (μM^{-1} s^{-1})
HIV-1	2.2	7.0	3.2
18.2 kDa HERV-K	10.3	0.8	0.1
11.6 kDa HERV-K	1.0	2.1	2.2

1C, lane 6). The 12 kDa protein was purified to homogeneity (Figure 1C, lane 7). N-Terminal sequencing confirmed that the 12 and 18.2 kDa precursor proteins autoprocessed at identical sites. Mass spectroscopy analysis demonstrated that the 12 kDa protein extended to the end of the engineered ORF at Met106, consistent with an expected molecular mass of 11 646 Da.

Both the 11.6 and 18.2 kDa forms of HERV-K PR specifically cleaved a fluorescent HIV PR peptide substrate, Lys-Ala-Arg-Val-Tyr-Phe(NO_2)-Glu-Ala-Nle-NH_2, derived from the p24-p2′ HIV-1 gag cleavage site sequence (Table 1). At pH 4.5 and 1 M NaCl, the K_m and k_{cat} values for the 11.6 kDa HERV-K enzyme were both slightly lower than those for HIV-1 PR, although the specificity constants, k_{cat}/K_m, were more similar. The K_m value for the 18.2 kDa form of HERV-K is about 1 order of magnitude higher than that for the 11.6 kDa form, while the k_{cat} is 2.5-fold lower. One possible explanation for the lower activity of the 18.2 kDa enzyme is that the unprocessed C-terminal amino acid extension acts as an inhibitor. Prolonged incubation of the 18.2 kDa PR at pH 6 and 37 °C resulted in cleavage of a 13-amino acid segment at the C terminus, supporting the notion that a region of the C terminus may act as a competitive "intramolecular substrate". This autocleavage was independent of the presence of the histidine tag on the C terminus (unpublished data). Similar results have been observed for the homologous protease from Mason-Pfizer monkey virus (*19*, *20*).

On the basis of the sequence similarity between HIV-1 and HERV-K PRs and on the basis of the ability of HERV-K PR to cleave an HIV-1 peptide substrate, one might expect cross-reactivity for inhibitors of these two enzymes. We tested a number of highly specific and potent HIV PR protease inhibitors (Figure 3), as well as the general aspartic

Table 2: Inhibition of Activity by Protease Inhibitors[a]

	K_i (nM) or % of inhibition at 10 μM		
inhibitor	HIV-1 PR	18.2 kDa HERV-K	11.6 kDa HERV-K
KNI227	0.037	15	4.6
KNI272	0.12	340	120.2
ABT538	0.032	415	60.2
Ro31-8959	0.54	9%	22%
Ro31-8624	3.6	0%	0%
L735,524	1.9	34%	35%
pepstatin A	24.8	48%	53%

[a] Each determination was repeated at least twice. Deviations from the mean value were less then 15%.

protease inhibitor, pepstatin A, for their ability to inhibit the 11.6 and 18.2 kDa forms of HERV-K PR. Both forms of HERV-K PR were highly resistant to all the HIV-1 PR inhibitors tested, including L-735,524 (indinavir), Ro31-8959 (saquinavir), and ABT-538 (ritonavir) which are currently used in antiretroviral treatments for AIDS (Table 2). The most potent inhibitor tested against HERV-K PR was KNI-227 with K_i values of 15 and 4.6 nM against the 18.2 and 11.6 kDa forms, respectively. The presence of the two methylene groups on the thioproline ring of KNI-227 seems to be more critical for binding to HERV-K PR than to HIV-1 PR (compare KNI-227 and KNI-272, Table 2). All the inhibitors tested were slightly more potent against the 11.2 kDa form of HERV-K PR, consistent with the lower K_m values obtained for the 11.2 kDa form.

Comparison of the model of HERV-K PR with the structure of HIV PR showed that there are a number of substitutions in residues that are predicted to define the subsite binding pockets, for example, V32L, V82L, I84L, G48T, and I50L (HIV-1 PR numbering). Interestingly, most of the sequence changes in the active site region occur at sites where drug resistance-conferring mutations have been observed for HIV-1 PR (*21*). These differences are expected to result in different specificities between the HIV-1 and HERV-K PRs, although it is difficult to ascribe K_i differences to specific residue changes in the absence of structural data. In contrast, the ability of HERV-K PR to recognize and cleave an HIV PR substrate was unexpected.

Dimeric Nature of the 11.6 kDa Form of HERV-K PR. The aggregation state of the 11.6 kDa form of HERV-K PR was investigated using sedimentation equilibrium analysis. A global fit of six data sets obtained using three rotor speeds with two different initial protein concentrations yielded a weight average molecular mass of 16 471 Da under near physiological conditions (pH 7.0 and 0.2 M NaCl). This value is higher than the molecular mass of the monomer (11 646 Da) but lower than that predicted for a dimer (23 292 Da). The data fit well to a monomer−dimer equilibrium model with a dissociation constant of 52.5 μM for the monomer or 0.61 mg/mL; good agreement was obtained between experimental data and simulated radial distribution curves of protein concentrations (Figure 4). Compared with the dimer dissociation constant of 0.1 mg/mL for HIV-1 PR under the same conditions (D. Xie et al., in preparation), HERV-K PR is a less stable dimer.

pH Dependence of the Activity and Stability of the 11.6 kDa PR. The pH and ionic strength dependence of enzyme activity for the 11.6 kDa form of HERV-K PR was compared to that for HIV-1 PR, whose activity is known to be highly

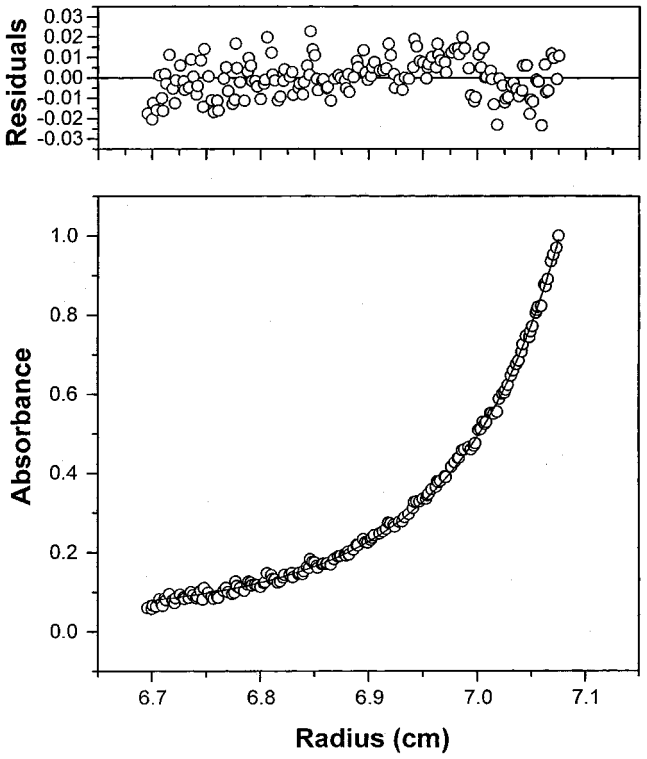

FIGURE 4: Sedimentation equilibrium analysis of HERV-K PR at pH 7.0 and 4 °C. (Top) The residual differences between the fitted curve and the experimental data. (Bottom) Absorbance at 280 nm as a function of centrifugal radius. The open circles represent the experimental data, and the solid line is the global fit of nine data sets using a monomer−dimer model. The monomer molecular weight used in the global analysis is 11 646. The obtained dissociation constant is a monomer concentration of 52.5 μM.

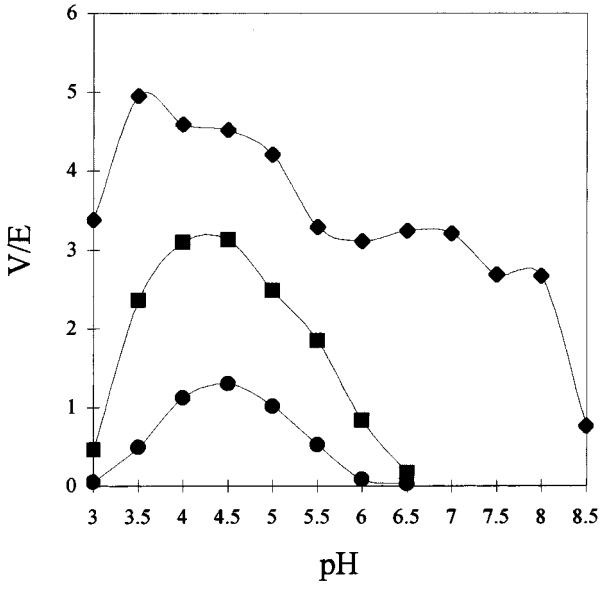

FIGURE 5: pH optimum activity of HERV-K10 PR. Activity was measured in different buffers without salt (circles) or in the presence of 1 M NaCl (squares) and 1.25 M ammonium sulfate (diamonds) as described in Materials and Methods. The initial velocity of substrate cleavage normalized for the enzyme (V/E) concentration was plotted as a function of pH.

sensitive to these parameters. At low ionic strengths (I = 0.02−0.05), the pH profile of HERV-K PR activity is bell-shaped with a peak at pH ~4.5 (Figure 5). The bell shape of the curve likely reflects the ionizations of the two catalytic

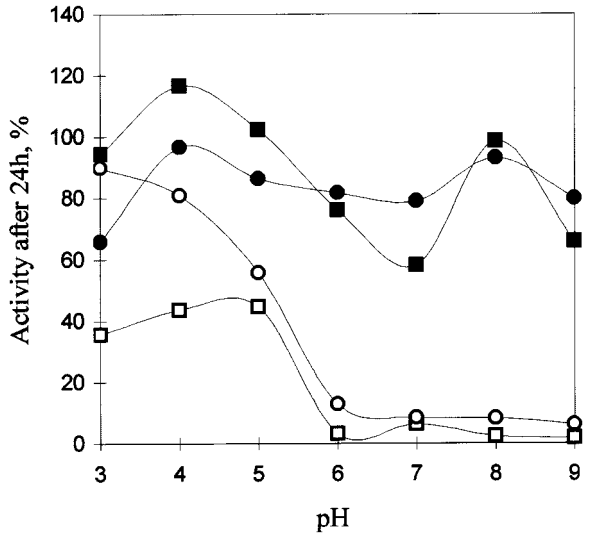

FIGURE 6: pH dependence of HERV-K10 and HIV-1 PR stability. HERV-K10 PR (black symbols) and HIV-1 PR (white symbols) were incubated at different pHs for 24 h without salt (circles) and in the presence of 1 M NaCl (squares). Residual activity was then measured at pH 6.2 at 1.25 M ammonium sulfate and plotted as a percentage of the original activity before the incubation.

carboxyl groups of the aspartic acid residues with estimated pK_a's of ~3.5 and 5.5. At a high ionic strength (1.0 M NaCl), enzyme activity was elevated at all pH levels but the shape of the curve was similar to that at low salt levels. The enzyme activity of HERV-K PR also shows a strong dependence on the nature of the salt as exhibited by the pH curve in 1.25 M ammonium sulfate. The salt dependence of HERV-K PR activity was similar to that described for HIV-1 PR and has been attributed to a "salting-out" effect which should stabilize hydrophobically driven interactions between the substrate and PR and may increase dimer stability (*22*, *23*). The greater extent of activation of HERV-K PR by sulfate versus chloride anion is consistent with the relative salting-out effectiveness of anions given by the Hofmeister series.

More than 60% of the HERV-K PR enzyme activity could be recovered after prolonged incubation at room temperature over a broad range of pH in the presence and absence of 1 M NaCl (Figure 6). In contrast, HIV-1 PR loses nearly all of its activity upon incubation at pH ≥6.0. HIV-1 PR is known to undergo autolysis and subsequent loss of activity (*24*, *25*), which may explain its lower stability. At pH 6.0, the 11.6 kDa form of HERV-K PR showed no apparent autolysis after prolonged incubation (data not shown). Interestingly, the stability of HERV-K PR at acidic pH is increased in the presence of 1 M NaCl, while that of HIV-1 PR is decreased in salt (Figure 6). The opposing salt effects on enzyme stability are consistent with the enhancing effect of NaCl on enzyme activity for HIV-1 PR which leads to greater autolysis during prolonged incubation.

Processing of HIV-1 Matrix-Capsid Protein by HERV-K PR. The fact that HERV-K PR is relatively insensitive to a variety of HIV-1 inhibitors combined with the fact that it appears to be expressed in a number of tissues (*1*, *6*) raises the possibility that the endogenous protease may somehow aid HIV-1 replication during highly active retroviral therapy. This hypothesis requires that HERV-K PR recognize and accurately process HIV-1 polyproteins. Previously, it was reported that the *E. coli*-expressed HERV-K PR could not cleave HIV-1 gag protein (*5*). However, these experiments were carried out using crude lysates. We decided to test the ability of the purified 11.6 kDa form of HERV-K PR to process a recombinant HIV-1 gag polyprotein consisting of the matrix and capsid domains (p17−p24), which contains one of the HIV-1 protease processing sites. SDS−PAGE analysis showed that purified HERV-K and HIV-1 PRs both cleave the p17−p24 polyprotein in a time-dependent fashion, although the HERV-K PR was less efficient (Figure 7). The two major cleavage products from the HERV-K PR digest were identified by mass spectroscopy and amino-terminal sequencing as mature p17 matrix and p24 capsid proteins that resulted from a single cleavage at the authentic SQNY−PIVQ cleavage site. Taken together, our results suggest that HERV-K PR may possess sufficient activity to complement HIV-1 PR under conditions where the latter activity is impaired due to either the presence of drug resistance mutations or the presence of a potent inhibitor. The ability of HERV-K PR to process other HIV-1 PR polyprotein cleavage sites, along with other possible complementation mechanisms, is currently under investigation.

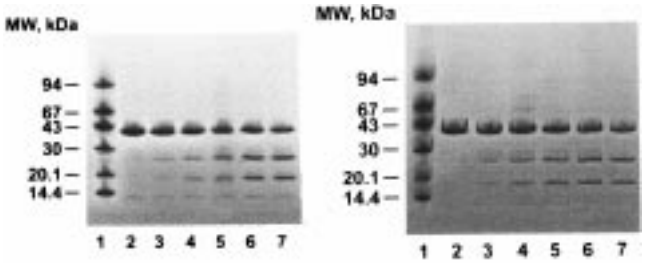

FIGURE 7: HIV-1 matrix-capsid protein cleavage by 11.2 kDa HERV-K (left) and HIV-1 PR (right) analyzed by Coomassie staining of 8 to 25% SDS−PAGE. Matrix-capsid protein at 1 mg/mL was incubated in 50 mM MES/NaOH buffer (pH 6.0) with the indicated proteases for 0, 10, 30, 120, and 180 min (lanes 2−7, respectively). In lane 1 are shown molecular weight markers.

ACKNOWLEDGMENT

We acknowledge Dr. Genesh Sathe and Mrs. Stefanie Van Horn for oligonucleotide synthesis and DNA sequencing, Mr. Dean McNulty of SmithKline Beecham Pharmaceuticals for technical assistance in peptide sequencing and mass spectroscopy, Mrs. Lisa Wysocki of SmithKline Beecham Pharmaceuticals for kindly providing the LW29(DE3) expression strain, Mr. Young Kim of the Protein Chemistry Lab (SAIC Frederick) for N-terminal sequencing of the matrix-capsid cleavage products, Mrs. Yu Chun Zhou of the Protein Chemistry Laboratory (SAIC Frederick) for technical assistance, Dr. Robert Fisher (Head of Protein Chemistry Laboratory, SAIC Frederick) for continuing support and useful conversation, Drs. Manal Swairjo and Trudy Smith of SmithKline Beecham Pharmaceuticals and Dr. Patricia Hoffman Towler of SAIC Frederick for critical reading of the manuscript, and Dr. Mike Eissenstat (SAIC Frederick) for kindly preparing Figure 3. The content of this publication does not necessarily reflect the views or policies of the Department of Health and Human Services, nor does mention of trade names, commercial products, or organization imply endorsement by the U.S. Government.

REFERENCES

1. Lower, R., Lower, J., and Kurth, R. (1996) *Proc. Natl. Acad. Sci. U.S.A 93*, 5177−5184.
2. Tonjes, R. R., Lower, R., Boller, K., Denner, J., Hasenmaier, B., Kirsch, H., Konig, H., Korbmacher, C., Limbach, C., Lugert, R., Phelps, R. C., Scherer, J., Thelen, K., Lower, J., and Kurth, R. (1996) *J. Acquired Immune Defic. Syndr. Hum. Retrovirol. 13* (Suppl. 1), S261−S267.
3. Ono, M., Yasunaga, T., Miyata, T., and Ushikubo, H. (1986) *J. Virol. 60*, 589−598.
4. Coffin, J. M., Hughes, S. H., and Varmus, H. E. (1997) *Retroviruses*, Cold Spring Harbor Laboratory Press, Plainview, NY.
5. Schommer, S., Sauter, M., Krausslich, H. G., Best, B., and Muellerlantzsch, N. (1996) *J. Gen. Virol. 77*, 375−379.
6. Benson, D. A., Boguski, M. S., Likpman, D. J., and Ostell, J. (1997) *Nucleic Acids Res. 25*, 1−6.
7. Simpson, G. R., Patience, C., Lower, R., Tonjes, R. R., Moore, H. D. M., Weiss, R. A., and Boyd, M. T. (1996) *Virology 222*, 451−456.
8. Tonjes, R., Boller, K., Limbach, C., Lugert, R., and Kurth, R. (1997) *Virology 233*, 280−291.
9. Sambrook, J., Fritsch, E. F., and Maniatis, T. (1989) *Molecular Cloning: A Laboratory Manual*, 2nd ed., Cold Spring Harbor Laboratory Press, Plainview, NY.
10. Genetics Computer Group, Inc. (1997) Madison, WI.
11. Towler, E. M., Stebbins, J. W., and Debouck, C. (1996) *Gene 183*, 259−263.
12. Gulnik, S. V., Suvorov, L. I., Liu, B., Yu, B., Anderson, B., Mitsuya, H., and Erickson, J. W. (1995) *Biochemistry 34*, 9282−9287.
13. Kageyama, S., Mimoto, T., Murakawa, Y., Nomizu, M., Ford, H., Jr., Shirasaka, T., Gulnik, S., Erickson, J., Takada, K., Hayashi, H., et al. (1993) *Antimicrob. Agents Chemother. 37*, 810−817.
14. Peranteau, A. G., Kuzmic, P., Angell, Y., Garcia-Echeverria, C., and Rich, D. H. (1995) *Anal. Biochem. 227*, 242−245.
15. Johnson, M. L., and Frasier, S. G. (1985) *Methods Enzymol. 117*, 301−342.
16. Zamyatnin, A. A. (1972) *Prog. Biophys. Mol. Biol. 24*, 107−123.
17. Stebbins, J., and Debouck, C. (1994) *Methods Enzymol. 241*, 3−16.
18. Rao, J. K., Erickson, J. W., and Wlodawer, A. (1991) *Biochemistry 30*, 4663−4671.
19. Zabransky, A., Andreansky, M., Hruskova-Heidingsfeldova, O., Havlicek, V., Hunter, E., Ruml, T., and Pichova, I. (1998) *Virology 245*, 250−256.
20. Hruskova-Heidingsfeldova, O., Andreansky, M., Fabry, M., Blaha, I., Strop, P., and Hunter, E. (1995) *J. Biol. Chem. 270*, 15053−15058.
21. Erickson, J. W. (1995) *Nat. Struct. Biol. 2*, 523−529.
22. Darke, P. L., Jordan, S. P., Hall, D. L., Zugay, J. A., Shafer, J. A., and Kuo, L. C. (1994) *Biochemistry 33*, 98−105.
23. Pargellis, C. A., Morelock, M. M., Graham, E. T., Kinkade, P., Pav, S., Lubbe, K., Lamarre, D., and Anderson, P. C. (1994) *Biochemistry 33*, 12527−12534.
24. Mildner, A. M., Rothrock, D. J., Leone, J. W., Bannow, C. A., Lull, J. M., Reardon, I. M., Sarcich, J. L., Howe, W. J., Tomich, C. S., Smith, C. W., et al. (1994) *Biochemistry 33*, 9405−9413.
25. Tomasselli, A. G., Mildner, A. M., Rothrock, D. J., Sarcich, J. L., Lull, J., Leone, J., and Heinrikson, R. (1995) *Adv. Exp. Med. Biol. 362*, 473−477.
26. Baldwin, E. T., Bhat, T. N., Gulnik, S., Liu, B., Topol, I. A., Kiso, Y., Mimoto, T., Mitsuya, H., and Erickson, J. W. (1995) *Structure 3*, 581−590.
27. Molecular Applications Group (1995) Massachusetts Institute of Technology, CERN, Palo Alto, CA.

BI9818927